Journal of NeuroVirology, 10: 255–259, 2004

ISSN: 1355-0284 print / 1538-2443 online
DOI: 10.1080/13550280490463479

Taylor & Francis
Taylor & Francis Group

Short Communication

In vivo monitoring of acute flavivirus (Modoc) encephalitis with regional and whole-brain quantitative diffusion magnetic resonance imaging

Johann Sellner,[1,3] Pieter Leyssen,[4] Sabine Heiland,[2] Philipp Rau,[1,3] Johan Neyts,[4] Francisco Martinez-Torres,[1,3] Peter Schramm,[2] Werner Hacke,[1] and Uta Meyding-Lamadé[1,3]

[1]Departments of Neurology and [2]Neuroradiology, and [3]Otto-Meyerhof-Zentrum, Ruprecht-Karls-University Heidelberg, Heidelberg, Germany; [4]Rega Institute for Medical Research, Katholieke Universiteit, Leuven, Belgium

In vivo **imaging of structural changes in the brain of patients with encephalitis has become an important aid in diagnostic and therapeutic procedures. Diffusion-weighted magnetic resonance imaging (DWI) was employed to quantitate regional and whole-brain diffusion-weighted MRI changes in a hamster model for acute flavivirus encephalitis. The regional apparent diffusion coefficient (ADC) was determined in hyperintense regions seen on T2-weighted images (i.e., the thalamic area and the temporal lobe), but anatomical variation and structural heterogeneity of encephalitic lesions severely impeded the placement of regions of interest (ROI). Therefore, quantitative whole-brain diffusion-weighted imaging was carried out and revealed a significantly reduced ADC ($P = .02$) in the brain of hamsters with acute encephalitis ($n = 7$) as compared to that of healthy, uninfected controls ($n = 3$). Furthermore, the ADC histogram demonstrated a reduced peak height and center of gravity during the acute encephalitis. Our findings could further support the use of diffusion-weighted imaging for *in vivo* monitoring of acute flavivirus encephalitis and for the study of therapeutic approaches.** *Journal of NeuroVirology* (2004) **10,** 255–259.

Keywords: diffusion-weighted imaging; encephalitis; flavivirus; magnetic resonance imaging

Worldwide, flaviviruses are a major cause of severe encephalitis in man, and the disease frequently progresses into coma and death (Campbell *et al*, 2002). Flaviviruses are mainly transmitted by the bite of an arthropod vector, especially mosquitoes. Prominent members of these enveloped, positive single-stranded RNA viruses belong to the Japanese encephalitis complex, such as the West Nile virus (WNV), Japanese encephalitis virus (JEV), Saint Louis encephalitis virus (SLEV), and Murray Valley encephalitis virus (MVEV) (Billoir *et al*, 2000; Kuno *et al*, 1998). The dramatic appearance of WNV encephalitis in the New York City Metropolitan area in late 1999 demonstrated that epidemics are not only restricted to rural areas of Africa and the Middle East. During the New York epidemic, 63% of the patients had clinical signs of encephalitis and 12% died (Nash *et al*, 2001). The subsequent appearance of WNV throughout the eastern states of the USA emphasizes quick spread by its natural host, primarily viremic birds, and its vector, the mosquito. Despite the clinical impact of flavivirus infections, there is as yet no effective therapy (Whitley and Gnann, 2002). Preventive measures include vector avoidance and mosquito control programs.

Recently, a convenient animal model for the study of flavivirus encephalitis in small laboratory rodents employing a flavivirus with low pathogenicity for man, i.e., the Modoc virus (MODV) (Leyssen *et al*, 2001), was introduced. The MODV has initially been isolated from a white-footed deer mouse in Modoc

Address correspondence to Johann Sellner, MD, Department of Neurology, Ruprecht-Karls-University Heidelberg, Im Neuenheimer Feld 400, D-69120 Heidelberg, Germany. E-mail: jsellner@arcor.de

This work was partly supported by a grant from the Forschungskommission der Medizinischen Fakultät, Ruprecht-Karls-University Heidelberg, Germany, to JS.

Received 29 April 2003; accepted 9 October 2003.

county, California, 1958, and seroconversion in rural inhabitants indicates natural infection without disease (Johnson, 1967; Zarnke and Yuill, 1985). However, intranasal as well as intraperitoneal inoculation of immunocompetent hamsters with MODV results in severe encephalitis mimicking the clinical symptoms and neuroradiological features as observed in patients with severe flavivirus encephalitis (Leyssen *et al*, 2003).

Magnetic resonance imaging (MRI) has become an important aid for the *in vivo* diagnosis of pathological brain conditions. Recently, cranial MRI has proven to be a highly sensitive tool for the *in vivo* monitoring of acute experimental encephalitis, such as that induced by herpes simplex virus, and the images obtained correlated well with the observed histopathology (Meyding-Lamadé *et al*, 1998; Thomas *et al*, 2001). In particular diffusion-weighted magnetic resonance imaging (DWI), which is a novel imaging technique based on the random translational movement of water in biological tissues, provides the opportunity to assess *in vivo* neuropathological changes at the molecular level (Cercignani and Horsfield, 2001). The initial clinical application of DWI has been in the diagnosis and prognosis of acute brain infarction. Recently, DWI was also shown to be more sensitive for the detection of changes due to cerebral infections as compared to conventional MRI (Teixeira *et al*, 2001).

We conducted this study to assess the usefulness of this upcoming imaging technique for the study of the pathogenesis and, whenever available in the future, the study of options for the treatment of flavivirus encephalitis. We determined whether the neuropathological changes induced by experimental flavivirus encephalitis can be differentiated employing DWI. To this end, the apparent diffusion coefficient (ADC) was calculated in regions of interest (ROIs) that we defined on conventional transverse relaxation time (T2)-weighted images. Unlike experimental brain infarction, encephalitic processes vary considerably intra- and interindividually in localization and extent. We therefore also determined the quantitative whole-brain ADCs and calculated pixel histograms obtained from the diffusion-weighted images.

Eight- to 12-week-old Gold hamsters (*Mesocricetus auratus*; breeder: Rega Institute, Belgium) were used throughout the experiments. The hamsters were maintained under artificial diurnal lighting conditions with free access to food and water. The principles of good laboratory animal care were followed. All experiments were approved by the ethical committee on vertebral animal experiments of the Katholieke Universiteit, Leuven. The detailed procedures on virus propagation, inoculation, and clinical observations were described recently (Leyssen *et al*, 2001). Briefly, seven hamsters were inoculated via the intranasal route with 10^4 PFU (plaque forming units) of MODV following a brief anesthesia. Negative controls (n = 3) received phosphate-buffered saline (PBS) instead. The animals received daily a single dose of 16 mg/kg of oxytetracycline by subcutaneous (s.c.) injection to suppress concomitant bacterial infection in the gut.

At day 13 post inoculation, the animals were anesthesized by intramuscular injection with a volume (2 μl/g) of a 1:2:2 mixture of atropine (0.5 mg/ml, 0.2 mg/kg; Sterop, Brussels, Belgium), ketamine (50 mg/ml, 40 mg/kg, Ketalar; Parke-Davis, Zaventem, Belgium), and xylazine (20 mg/ml, 16 mg/kg, XYL-M 2%; VMD, Arendonk, Belgium). The MRI scans were generated with a 2.35-tesla scanner (Bruker Medizintechnik, Ettlingen, Germany). An MRI protocol was used consisting of a diffusion-weighted spin-echo echo-planar imaging (SE-EPI) sequence (repetition time = 3 s; echo-time 63 ms; number of averages = 4; diffusion gradient duration (δ) = 5 ms; diffusion time (Δ) = 45 ms; *b*-values = 200, 300, 400, 500, 600, 700 s/mm^2; field of view = 4 cm × 4 cm; matrix = 128 × 64; number of slices = 6; slice thickness = 2 mm) and a multi-spin-echo sequence (repetition time = 3 s; 12 echoes with echo times of 8, 16, 24, ..., 96 ms; number of averages = 1; field of view = 4 cm × 4 cm; matrix = 256 × 128; number of slices = 6; slice thickness 2 mm). Image data were transferred to a SUN-Sparcstation 10 (Sun Microsystems, USA) for further offline processing.

On the T2-weighted images, hyperintensities were indicative for acute inflammation, i.e., the thalamic area and temporal lobe. Subsequently, we calculated the ADCs in the corresponding regions on diffusion-weighted images (Figure 1). The ADCs were derived from the diffusion-weighted data set by linear

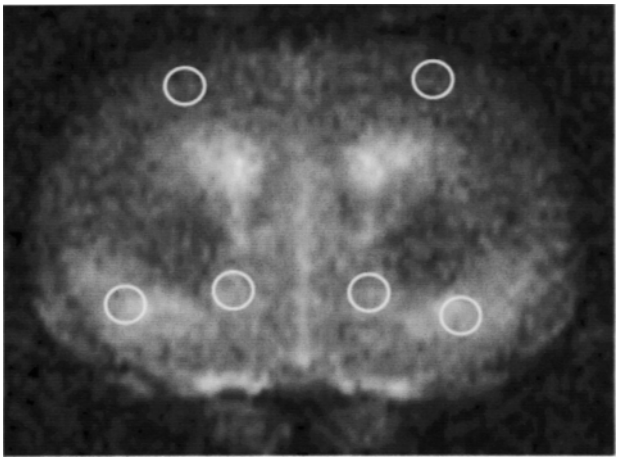

Figure 1 Coronal diffusion-weighted image of the brain of a hamster with severe, acute MODV encephalitis. Regions of interest (ROI) used for postprocessing are marked with circles. Thalamic and temporal lobe ROIs correspond to hyperintensities on T2-weighted images. The ROI in the parietal lobe was used as internal reference in terms of normal appearing white matter in absence of virus copies.

regression of ln($S(b)$), considering the relationship

$$S(b) = S_0{}^* \mathrm{e}^{-b^* \mathrm{ADC}}$$

with S_0 the signal intensity without diffusion weighting and $S(b)$ is the signal intensity at a b-value. Furthermore, also the T2 time was calculated from the multiecho data set by linear regression of ln(S(TE)), considering the relationship

$$S(\mathrm{TE}) = S_0{}^* \mathrm{e}^{-\mathrm{TE/T2}}$$

where S is the signal intensity and TE is the echo time.

In a second step the brain was manually segmented on all slices. Entire ADC maps were obtained on a pixel-by-pixel basis. From these ADC maps, a frequency histogram was created showing the number of pixels with ADC in certain ranges. The ADC histogram was determined in steps of 50×10^{-6} mm^2/s. For statistical testing, the Student's t test with $P < .05$ was considered to be significant.

All of the intranasally infected hamsters that were used in this study developed observable clinical symptoms, such as paralysis and tremor, suggestive of moderate to severe meningoencephalitis. The brain of these hamsters showed lesions with a specific and recurrent topographic distribution pattern on the T2-weighted images and were predominantly located in morphological areas belonging to the olfactory-limbic system, such as the olfactory bulbs, thalamic area, temporal lobes, amygdaloid area, and the hippocampus. All animals survived the MRI imaging procedure and were euthanized afterwards. Histopathological examination of the brains in the affected regions revealed fulminant infiltration by inflammatory cells and massive tissue destruction.

First, we selected sites with high signal intensity on T2-weighted images that also showed signs of extensive neuropathology upon histological examination. The selected areas were located in the temporal lobe and the thalamic area (Figure 1). As an internal reference of normal appearing white matter, we examined the parietal lobe due to the absence of histopathological abnormalities and virus copies. There were no significant differences on statistical tests in the ADCs when comparing the data from the two hemispheres. The data for the regional ADC-values are shown in Table 1. All regions assessed in the animals with acute MODV encephalitis showed reduced ADCs as compared to healthy, uninfected controls. However, for none of the selected regions a statistically significant ADC reduction was observed ($P > .05$).

In a second step, we calculated the mean ADC using data derived from whole-brain measurements. The mean whole-brain ADC in animals with acute MODV encephalitis was calculated to be $(693.1 \pm 90.0) \times 10^{-6}$ mm^2/s, which is significantly lower as compared to those observed in healthy, uninfected controls, i.e., with $(775.5 \pm 35.5) \times 10^{-6}$ mm^2/s ($P = .02$). We constructed an ADC/pixel histogram derived from the whole-brain images of both groups (Figure 2). Here, animals with acute MODV encephalitis presented a decreased peak height as well as a shift of the curve to lower ADC values. The center of gravity of the curve was shifted from 662.61×10^{-6} mm^2/s in healthy, uninfected controls to 628.74×10^{-6} mm^2/s for hamsters with acute encephalitis (Table 2).

Table 1 Regional DWI in healthy, uninfected controls (n = 3) and in hamsters with acute MODV encephalitis (n = 7)

	Parietal cortex	*Temporal lobe*	*Thalamic area*
Healthy controls	659.1 ± 22.5	631.1 ± 13.1	674.5 ± 26.8
Acute encephalitis	611.4 ± 67.2	610.7 ± 98.3	672.9 ± 119.6
t test	$P = .14$	$P = .37$	$P = .49$

Mean ADC values ± standard deviation (SD) in regions of interest are given. Values are shown as $\times 10^{-6}$ mm^2/s.

In the present study, we investigated the usefulness of DWI for the study of neuronal tissue abnormalities in an experimental *in vivo* model for acute flavivirus encephalitis. To our knowledge, this study represents the first in which regional ADC levels and whole-brain quantitative ADC maps are used for this purpose.

The general clinical hallmark of acute viral encephalitis is a triad of fever, headache, and altered consciousness. Other symptoms can be behavioral and speech disturbances, focal and diffuse neurological signs, such as hemiparesis or seizures (Whitley and Gnann, 2002). Therapy of viral encephalitis, with exception of herpesvirus-induced encephalitis, is mainly limited to intensive supportive care. Therefore, the development of improved monitoring tools, as well as novel therapies are essential. DWI is a promising technique to study abnormalities at the cellular and subcellular level in living subjects, because its principle is based on the random translational motion (diffusion) of water molecules

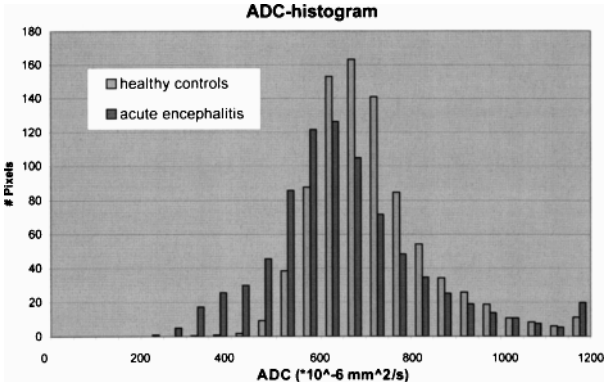

Figure 2 ADC histogram derived from the whole-brain diffusion-weighted MR images (DWI) in case of healthy, uninfected controls (n = 3) and hamsters with acute MODV encephalitis (n = 7). A two-tailed, gaussian distribution is observed in both groups with a decreased maximum and an apparent shift to the left of the curve derived for hamsters with acute MODV encephalitis as compared to that of the healthy, uninfected controls.

Table 2 Quantitative whole-brain DWI in healthy, uninfected controls (n = 3) and in hamsters with acute MODV encephalitis (n = 7)

	Peak height	*Mean ADC*	*Center of gravity*
Healthy controls	163.17 ± 40.97	775.5 ± 35.5	662.61
Acute encephalitis	126.14 ± 20.28	693.1 ± 90.0	628.74
t test		$P = .02$	

Peak height ± SD, mean ADC ± SD, and center of gravity of the ADC histogram (see also Figure 2) are given. Values are shown as $\times 10^{-6}$ mm^2/s.

in tissues. Quantitation is possible by applying different magnetic field gradients of diffusion sensation, allowing the calculation of the ADC (Le Bihan, 1991). DWI has proven to be a highly sensitive tool for the diagnosis of structural damage in central nervous system disorders. The ability to obtain early and highly specific information has made DWI an important tool in clinical assessment of hyperacute cerebral ischemia (Schellinger *et al*, 2001). Advanced knowledge of infarct pathogenesis following examination with DWI allows us to assess the outcome of therapy, such as fibrinolysis, in treated patients (Lovblad *et al*, 1997; Rother *et al*, 2002). So far, little is known about the usefulness of DWI in the diagnosis and prognosis of acute viral encephalitis. However, hands-on diagnosis and early initiation of adequate therapy is vital to improve the outcome of the disease. Most viruses have predilection sites, but evolution of the lesions and correlation with symptoms differ widely (Whitley and Gnann, 2002). Furthermore, as has been observed for WNV, some viruses may have a fatal outcome, although, as shown by the autopsy of New York epidemic cases, only minimal cerebral inflammation was present (Shieh *et al*, 2000). Quantitative whole-brain measurement of the changes induced by the disease could provide an approach towards better *in vivo* monitoring of the course of acute encephalitis in patients.

Our results indicate that distinct water diffusion changes occur in acute encephalitis and reflect the ongoing pathophysiology. As in our study, decreased ADC values were reported in diseased brain regions of patients with viral encephalitis (i.e., induced by herpes simplex virus) (Sener, 2001, 2002). Although a reduced ADC was observed in diseased brain regions, anatomical variation and the structural heterogeneity of encephalitic lesions severely impeded the placement of ROI. Despite lower ADC values in diseased areas such as the thalamic region and the temporal lobe, the water diffusion changes were not significant. Even within the internal reference, the parietal lobe, where no viruses were detected on histopathological examination, lower and highly variable values were noticed. This observation may reflect secondary, virus-independent mechanisms leading to tissue abnormalities but also difficulties in defining the area of interest. Therefore, to assess the overall burden of cerebral lesions, we pursued a more global approach by calculating whole-brain ADCs, and comparing ADC histograms by shape and center of gravity. The ADC histograms of healthy control animals were characterized by a gaussian distribution, with most of the ADC values measured in the cerebral volume concentrated within a small range (Figure 2). Also in case of animals with acute MODV encephalitis, ADC histograms were characterized by a gaussian distribution; however, (i) the peak height was significantly reduced (from 163.17 ± 40.97 to 126.14 ± 20.28 pixels), (ii) the mean quantitative whole-brain ADC was significantly ($P < .02$) reduced, and (iii) and the center of gravity was shifted significantly to lower values (from 662.61 to 628.74 $\times$ 10^{-6} mm^2/s). Taken together, the changes put forward by these data indicate that in the brain of animals with acute encephalitis, diffusion is markedly reduced in most of the pixels measured. The underlying pathological mechanisms that yield reduced ADCs in DWI are still under discussion. In case of acute viral encephalitis, as is presented in this study, cytotoxic edema may explain the observed changes. The drop of ADCs could be governed by the proinflammatory interleukin-1b, which was proven to be neurotoxic (Blamire *et al*, 2000). In inflammatory lesions, toxic inflammatory changes (induced/caused by cytokines, oxidative products, proteolytic enzymes) may induce mitochondrial dysfunction and lead to metabolic failure, thus causing a reduction of the ADC (Heales *et al*, 1999). In experimental models of epilepsy, metabolic changes leading to (i) an influx of water into cells, (ii) an excitatory over-activation, and (iii) increased glucose utilization stimulating anaerobic glycolysis are suggested to cause a reduction of the ADC (Blennow *et al*, 1985; Hoshi and Tamura, 1992).

The results reported in this study provide new insights in the *in vivo* pathophysiology of viral encephalitis, in particular that caused by flaviviruses. As demonstrated by Teixeira *et al* (2001), the application of DWI for the diagnosis and study of herpes simplex virus encephalitis provided a technique that allows earlier and more sensitive detection of lesions, as well as a better understanding of the nature of the lesions than is possible based on T2-weighted images alone. For this reason, longitudinal studies with DWI combining regional and whole brain quantitative DWI could provide further information. Furthermore, microstructural alterations can progress after encephalitis despite clinical recovery, as seen in herpes encephalitis (Meyding-Lamadé *et al*, 1999; Mitsufuji and Ikuta, 2002). This should also be taken in account for monitoring acute encephalitis at later stages of disease and for the distinction of possible relapses.

In conclusion, the present study demonstrates that acute experimental flavivirus (MODV) encephalitis is associated with water diffusion changes in the brain as detected by DWI, an advanced technique that allows *in vivo* monitoring of the disease and in

particular to examine the nature of the brain lesions. Currently, there still does not exist an effective strategy for the treatment of flavivirus-induced encephalitis, either by inhibiting viral replication in the brain or by relieving severe clinical symptoms (Campbell *et al*, 2002). Further studies in animal models and patients will be required to examine whether DWI provides a useful method for *in vivo* monitoring of flavivirus encephalitis and novel therapeutic approaches thereof.

References

Billoir F, de Chesse R, Tolou H, de Micco P, Gould EA, de Lamballerie X (2000). Phylogeny of the genus flavivirus using complete coding sequences of arthropod-borne viruses and viruses with no known vector. *J Gen Virol* **81 (Pt 9):** 2339.

Blamire AM, Anthony DC, Rajagopalan B, Sibson NR, Perry VH, Styles P (2000). Interleukin-1beta-induced changes in blood-brain barrier permeability, apparent diffusion coefficient, and cerebral blood volume in the rat brain: a magnetic resonance study. *J Neurosci* **20:** 8153–8159.

Blennow G, Nilsson B, Siesjo BK (1985). Influence of reduced oxygen availability on cerebral metabolic changes during bicuculline-induced seizures in rats. *J Cereb Blood Flow Metab* **5:** 439–445.

Campbell GL, Marfin AA, Lanciotti RS, Gubler DJ (2002). West Nile virus. *Lancet Infect Dis* **2:** 519–529.

Cercignani M, Horsfield MA (2001). The physical basis of diffusion-weighted MRI. *J Neurol Sci* **186 (Suppl 1):** S11–S14.

Heales SJ, Bolanos JP, Stewart VC, Brookes PS, Land JM, Clark JB (1999). Nitric oxide, mitochondria and neurological disease. *Biochim Biophys Acta* **1410:** 215–228.

Hoshi Y, Tamura M (1992). Cerebral oxygenation state in chemically-induced seizures in the rat—study by near infrared spectrophotometry. *Adv Exp Med Biol* **316:** 137–142.

Johnson HN (1967). Ecological implications of antigenically related mammalian viruses for which arthropod vectors are unknown and avian associated soft tick viruses. *Jpn J Med Sci Biol* **20:** 160–166.

Kuno G, Chang GJ, Tsuchiya KR, Karabatsos N, Cropp CB (1998). Phylogeny of the genus Flavivirus. *J Virol* **72:** 73–83.

Le Bihan D (1991). Molecular diffusion nuclear magnetic resonance imaging. *Magn Reson Q* **7:** 1–30.

Leyssen P, Croes R, Rau P, Heiland S, Verbeken E, Sciot R, Paeshuyse J, Charlier N, De Clerq E, Meyding-Lamadé U, Neyts J (2003). Acute encephalitis, a poliomyelitis-like syndrome and neurological sequelae in an hamster model fpr flavivirus infections. *Brain Pathol* **13:** 279–290.

Leyssen P, Van Lommel A, Drosten C, Schmitz H, De Clerq E and Neyts J (2001). A novel model for the study of the therapy of flavivirus infections using the modoc virus. *Virology* **279:** 27–37.

Lovblad KO, Baird AE, Schlaug G, Benfield A, Siewert B, Voetsch B, Connor A, Burzynski C, Edelman RR, Warach S (1997). Ischemic lesion volumes in acute stroke by diffusion-weighted magnetic resonance imaging correlate with clinical outcome. *Ann Neurol* **42:** 164–170.

Meyding-Lamadé U, Lamadé W, Kehm R, Knopf KW, Hess T, Gosztonyi G, Degen O, Hacke W (1998). Herpes simplex virus encephalitis: cranial magnetic resonance imaging and neuropathology in a mouse model. *Neurosci Lett* **248:** 13–16.

Meyding-Lamadé U, Lamadé W, Kehm R, Oberlinner C, Fäth A, Wildemann B, Haas J, Hacke W (1999). Herpes simplex virus encephalitis: chronic progressive cerebral MRI changes despite good clinical recovery and low viral load—an experimental mouse study. *Eur J Neurol* **6:** 531–538.

Mitsufuji N, Ikuta H (2002). Asymptomatic self-limiting white matter lesions in the chronic phase of herpes simplex encephalitis. *Brain Dev* **24:** 300–303.

Nash D, Mostashari F, Fine A, Miller J, O'Leary D, Murray K, Huang A, Rosenberg A, Greenberg A, Sherman M, Wong S, Layton M (2001). The outbreak of West Nile virus infection in the New York City area in 1999. *N Engl J Med* **344:** 1807–1814.

Rother J, Schellinger PD, Gass A, Siebler M, Villringer A, Fiebach JB, Fiehler J, Jansen O, Kucinski T, Schoder V, Szabo K, Junge-Hulsing GJ, Hennerici M, Zeumer H, Sartor K, Weiller C, Hacke W (2002). Effect of intravenous thrombolysis on MRI parameters and functional outcome in acute stroke <6 hours. *Stroke* **33:** 2438–2445.

Schellinger PD, Fiebach JB, Jansen O, Ringleb PA, Mohr A, Steiner T, Heiland S, Schwab S, Pohlers O, Ryssel H, Orakcioglu B, Sartor K, Hacke W (2001). Stroke magnetic resonance imaging within 6 hours after onset of hyperacute cerebral ischemia. *Ann Neurol* **49:** 460–469.

Sener RN (2001). Herpes simplex encephalitis: diffusion MR imaging findings. *Comput Med Imaging Graph* **25:** 391–397.

Sener RN (2002). Diffusion MRI in Rasmussen's encephalitis, herpes simplex encephalitis, and bacterial meningoencephalitis. *Comput Med Imaging Graph* **26:** 327–332.

Shieh WJ, Guarner J, Layton M, Fine A, Miller J, Nash D, Campbell GL, Roehrig JT, Gubler DJ, Zaki SR (2000). The role of pathology in an investigation of an outbreak of West Nile encephalitis in New York, 1999. *Emerg Infect Dis* **6:** 370–372.

Teixeira J, Zimmermann RA, Haselgrove JC, Bilaniuk LT, Hunter JV (2001). Diffusion imaging in pediatric central nervous system infections. *Neuroradiology* **43:** 1031–1039.

Thomas HC, Kapadia RD, Wells GI, Gresham AM, Sutton D, Solleveld HA, Sarkar SK, Dillon SB, Tal-Singer R (2001). Differences in pathogenicity of herpes simplex virus serotypes 1 and 2 may be observed by histopathology and high-resolution magnetic resonance imaging in a murine encephalitis model. *J NeuroVirol* **7:** 105–116.

Whitley RJ, Gnann JW (2002). Viral encephalitis: familiar infections and emerging pathogens. *Lancet* **359:** 507–513.

Zarnke RL, Yuill TM (1985). Modoc-like virus isolated from wild deer mice (Peromyscus maniculatus) in Alberta. *J Wildl Dis* **21:** 94–99.